Pretreatment with a β-cyclodextrin - corrosion inhibitor complex stops an initiated corrosion process on zinc

Abdulrahman Altin,[†] Ashokandand Vimalanandan,[†] Adnan Sarfraz,[†]

Michael Rohwerder,[†] and Andreas Erbe[*,†,‡]

[†]*Max-Planck-Institut für Eisenforschung GmbH, Max-Planck-Str. 1, 40237 Düsseldorf, Germany*

[‡]*NTNU, Norwegian University of Science and Technology, Department of Materials Science and Engineering, 7491 Trondheim, Norway*

E-mail: cd-pretreatment@the-passivists.org

Abstract

Metal pretreatment is typically the first step in a reliable corrosion protection system. This work explores the incorporation of complexes between the cyclic oligosaccharide β-cyclodextrin (β-CD) and the molecular organic corrosion inhibitor 2-mercaptobenzothiazole (MBT) into an oxide-based pretreatment layer on metallic zinc. The layers were produced by a precorrosion step in the presence of β-CD. Resulting films have a morphology dominated by spherical particles. X-ray photoelectron spectroscopy (XPS) investigations of the surfaces show the sulfur atoms of MBT to be partially oxidized but mostly intact. Samples pretreated with such a layer where subsequently coated with a model polymer coating, and the delamination of this model coating from an artificial defect was monitored by a scanning Kelvin probe (SKP). SKP results show

a slow down of delamination after several hours of the ongoing corrosion process for surfaces pretreated with the complexes. Finally, a lifting of the electrode potential in the defect was observed, with a subsequent complete stop in delamination and repassivation of the defect after ≈10 h. The repassivation is attributed to the release of MBT after initiation of the corrosion process. Most likely, the increase of pH, combined with the availability of aqueous solution, facilitates the MBT release after initiation of a corrosion process. Consequently, complexes formed from β-CD and corrosion inhibitors can be effectively incorporated into inorganic pretreatments, and the inhibitor component can be released upon start of the corrosion process.

Introduction

Corrosion of metallic structural materials can cause both environmental damage as well as financial losses.[1,2] An effective corrosion protection system for actively corroding metals typically starts with a pretreatment step.[3] The main functions of the metal pretreatment are to increase the resistance against corrosion and improve adhesion between metal and polymer coatings.[3,4] In general, a pretreatment process represents a short, accelerated corrosion process, which modifies the surface of the material such that further corrosion processes will be slowed down.[3] Technically relevant pretreatment concepts include phosphating,[3,5,6] oxide-based nanoceramic conversion coatings,[7] and chromating.[3,8–11] The latter is particularly effective, however, is based on Cr^{IV} and currently replaced by new methods because of Cr^{IV} toxicity and cancer-causing properties.[7,8,12] The main advantage of chromate-based systems in corrosion protection is the fact that chromate becomes available by hydrolysis, and is reduced during a corrosion process to Cr^{III}, leading to precipitation of a passivating oxide, and hence to a stop of the corrosion process.[9,11] While this "active" corrosion protection is beneficial, the system's main drawback is the uncontrolled release of the toxic Cr^{IV} without any corrosion attack.[10] It would be much more desirable to release the protective agents when corrosion occurs. Recent efforts to realize such triggered release focus e.g. on sophisticated

capsule-based concepts.[13,14] Possible triggers for such systems are pH change,[15,16] electrode potential change,[17] or ionic strength change.[18]

This work explores the use of complexes between the cyclic oligosaccharide β-cyclodextrin (β-CD) and the corrosion inhibitor mercaptobenziothiazole (MBT) [Figure 1] in pretreatment of zinc. These complexes are denoted in this work as β-CD[MBT]. MBT is a well-known corrosion inhibitor, amongst others for zinc and copper.[19] CDs are synthetic substances produced by enzymatic conversion of starch and are formed by 1-4 linked glucose units.[20–22] The native CD consists of 6, 7 or 8 glucose sub units and are designated as α-, β-, and γ-CD, respectively. Figure 1 shows the chemical and geometric structure of β-CD. Due to its geometrical arrangement it can be used as a host for organic compounds, e.g., in order to increase the solubility.[20,21] This host-guest chemistry opens up a wide range of applications for β-CD in different areas.[22]

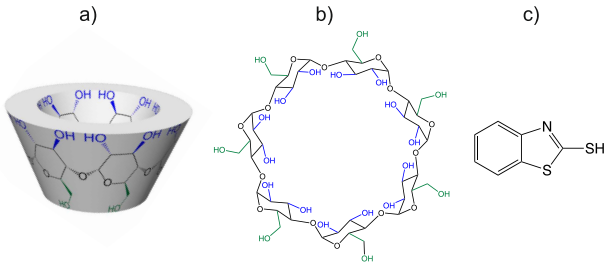

Figure 1: Structure of β-Cyclodextrin (β-CD); (a) chemical structure; (b) 3-D cone-like spatial arrangement. (c) Chemical structure of 2-mercpatobenzothiazole (MBT).

Few previous applications exist exploiting the host guest chemistry of CDs, in particular β-CD, in corrosion protection of metals. On 2024 aluminum alloy, complexes between β-CD and corrosion inhibitors have been incorporated into sol-gel derived organosilicate hybrid coatings, and a defect healing was found by scanning vibrating electrode measurements.[23] Performance of this concept increased when combined with an organic coating on the same aluminum alloy.[24] Later, more extensive studies basing on the same aluminum alloy have been conducted, testing several CDs.[25] The modification of chitosan with β-CD resulted in a reduced corrosion rate of carbon steel in hydrochloric acid compared to uncoated steel, where the chitosan-CD structure was described as inhibitor.[26] β-CD itself acts as corrosion

inhibitor for zinc in the presence of up to 0.1M chloride.[27]

Zinc is widely used as metallic coating for steels, and to a lesser extend also on aluminum alloys. As opposed to the situation investigated for one class of aluminum alloys in above mentioned works employing inhibitor release systems where localized corrosion is dominant,[23–25] uniform corrosion dominates corrosion of zinc.[28] Galvanized structures may be further protected by organic coatings. For these coatings, corrosion-driven cathodic delamination is one of the fastest failure processes in humid atmosphere.[29] Cathodic delamination is initiated from a defect in the coating. The mechanism of this process has been investigated extensively elsewhere.[30,31] Different approaches have been employed to slow down or stop this process. One way of slowing down cathodic delamination is strengthening the bond between the metal and the coating.[32] Another approach is adding corrosion inhibiting additives in the coating which are released in the case of corrosion occurs and stop the corrosion in the defect.[33,34] In a previous work, our group has shown that the incorporation of β-CD[MBT] complexes into model coatings leads to the stop of cathodic delamination by pH-triggered release of MBT.[35] A similar approach has more recently been shown to work on steels when the β-CD - inhibitor complex was bound to graphene.[36]

Incorporation into a polymer coating is not compatible with all types of polymeric systems. An incorporation of the inhibitor into a pretreatment is therefore an attractive alternative. Incorporation into a pretreatment is furthermore also suitable in the numerous applications where zinc is applied without organic coatings. In this work, a corrosion-like pretretment step in an β-CD[MBT] containing chloride solution is used to incorporate β-CD[MBT] into the oxide corrosion product forming on zinc. The resulting surfaces were characterised by scanning electron microscopy (SEM) and X-ray photoelectron spectroscopy (XPS). In a subsequent step, model polymer coatings have been deposited on top of the zinc layers, and the kinetics of their delamination from a prepared defect has been investigated by a scanning Kelvin probe (SKP).

Materials and Methods

Zinc sheets (99.95%) with a thickness of 1.5 mm bought from Goodfellow were cut in pieces of 15 mm × 20 mm and grounded with SiC grinding papers (1000P, 2500P, 4000P) and polished with a diamond polishing compound (1 µm). The specimens were cleaned with ethanol and dried under a nitrogen stream. The chemicals used, MBT, β-CD, KCl, poly(vinyl butyral-co-vinyl alcohol-co-vinyl acetate) (PVB) (M_{w}= 50000 - 80000 g mol^{-1}) were purchased from Sigma-Aldrich. Aqueous solutions were prepared with water from an USF ELGA water purification system (conductivity <0.055 µS cm^{-1}).

β-CD[MBT] was prepared by a route described previously,[35] on the basis of the commonly used suspension preparation.[37] The β-CD (2 g; 1.76 mmol) was suspended in 100 mL ultrapure water. Under vigorous stirring, the equimolar amount of MBT (295 mg) was added. The solution was stirred for at least 24 h at room temperature. The solution was subsequently centrifuged, and the obtained slightly yellow powder was dried at 50°C in vacuum for 24 h.

Preparation of the pretreatments was carried out by stirring fresh zinc specimens in 0.1M KCl solution containing 5mM of β-CD[MBT] complex for 24 h at room temperature. Two sets of control experiments were carried out. In the first set, zinc sheets were exposed to 0.1M KCl, while in the second set, the samples were exposed to 0.1M KCl containing 5mM β-CD. All samples were subsequently rinsed with water and dried under a nitrogen stream. A 10wt% solution of PVB in EtOH was applied afterwards, spin coated at 2500 rpm. The spin coating step was conducted twice. The so prepared model coatings were then dried for 30 min in an oven at 70°C and transferred directly to the SKP chamber. The samples were exposed at least for 1 h to the atmosphere in the SKP chamber at constant humidity to eliminate charging effects.

A commercial SKP system (KM Soft Control) was used to investigate the delamination process.[38] All potentials are referred to Standard Hydrogen Electrode (SHE). The NiCr-tip was calibrated prior the experiments with Cu/$CuSO_4$(sat.). The initiation of the delamina-

tion was done by scratching the samples with a scalpel. The defects created in this manner are about ≈3 mm long and 200 µm wide. The defect was covered afterwards with 7.5 µL 1M KCl solution. The SKP chamber was purged with humid air. The relative humidity in the chamber during the experiments was above 90%. Working principle and evaluation of SKP data is described elsewhere.[31] The position of the inflection point of the obtained potential profiles has been used as position of the delamination front, and its temporal progress has been analyzed.

For SEM, a Zeiss LEO 1550 VP system, combined with an Oxford Instruments 7426 energy-dispersive X-ray spectrometer (EDX) was used to investigate surface morphology and surface composition. Images were recorded at an acceleration voltage of 10 keV and at a working distance of 4-6 mm.

XPS (Quantera II, Physical Electronics, Chanhassen, MN, USA) was conducted to investigate the chemical composition of the pretreated surfaces. The monochromatic Al Kα X-ray source (1486.6 eV) was operated at a pass energy of 26 eV, a step size of 0.1 eV was used, and the measurement area was 100 µm × 100 µm. The take-off angle was 45°. The quantitative analysis was carried out with CasaXPS 2.3.15.[39] In addition to scientific literature indicated, generally available internet sources have been used in the interpretation of the obtained spectra.[40,41]

Results and Discussion

Surfaces of pretreated zinc

The surface morphology of the prepared zinc surfaces is shown in Figure 2. Figure 2a show a typical zinc surface after 24 h exposure to chloride containing electrolyte. Corrosion products on this surface are randomly and inhomogeneously distributed on the zinc surface. When adding 5mM β-CD to the solution, the surface shows a different morphology. As shown in Figure 2b, products exhibit a fiber-type connection between individual crystallites

of corrosion products. By adding 5mM β-CD[MBT] to the bath, another type of film is generated (Figure 2c). This film shows a particulate structure, with particles of a diameter of $\approx$1 µm.

The chemical composition of the films has been characterized by XPS. Figure 3 shows an overview of the obtained XP spectra. The survey spectrum (Figure 3a) shows the presence of the elements which are expected in the system, Zn, O, N, C, and S. The O 1s peak was not analyzed in detail, due to the fact that its internal structure is often hard to interpret. The oxygen content is originating from ZnO as well as β-CD. The C 1s peak in Figure 3b shows two main components, centered in this fit at 284.2 eV and 285.7 eV. The former peak indicates carbon involved in non-polar bonds (labeled C–C in Figure 3b), while the latter indicates carbon involved in polar bonds, such as with O or N atoms (labelled C–[polar]–C in Figure 3b). The C 1s spectrum confirms the presence of organic molecules at the surface, and is consistent with the presence of a significant amount of β-CD and MBT. A component corresponding to carbonate at higher binding energies has also been included in the analysis, however, no significant contributions of this component have been found. Consequently, the formation of zinc carbonate is not dominant under the conditions chosen in this work. The presence of sulfur and nitrogen in the obtained layer point to the presence of MBT in the layer.

The S 2p region of the XP spectrum (Figure 3d) can be described with three S $2p_{1/2}$ / S $2p_{3/2}$ doublets, showing that the system contains at least three chemically distinct sulfur species. Their S $2p_{3/2}$ components are centered at 162.9 eV, 164.7 eV and 168.8 eV. MBT (Figure 1c) contains two distinct sulfur atoms. Consequently, XPS of MBT shows two sulfur doublets with an intensity ratio of 1:1 at $\approx$162 eV and $\approx$164.5 eV.[42–45] The peak at the lower binding energy is assigned to the exocyclic S-atom, while the one at higher binding energy originates from the endocyclic S-atom.[42–45] The two lowest S 2p peaks observed here are hence also assigned to originate from MBT. The broad peak at 168.8 eV originates from oxidized sulfur. The broadness of this peak indicates that different oxidized forms of sulfur

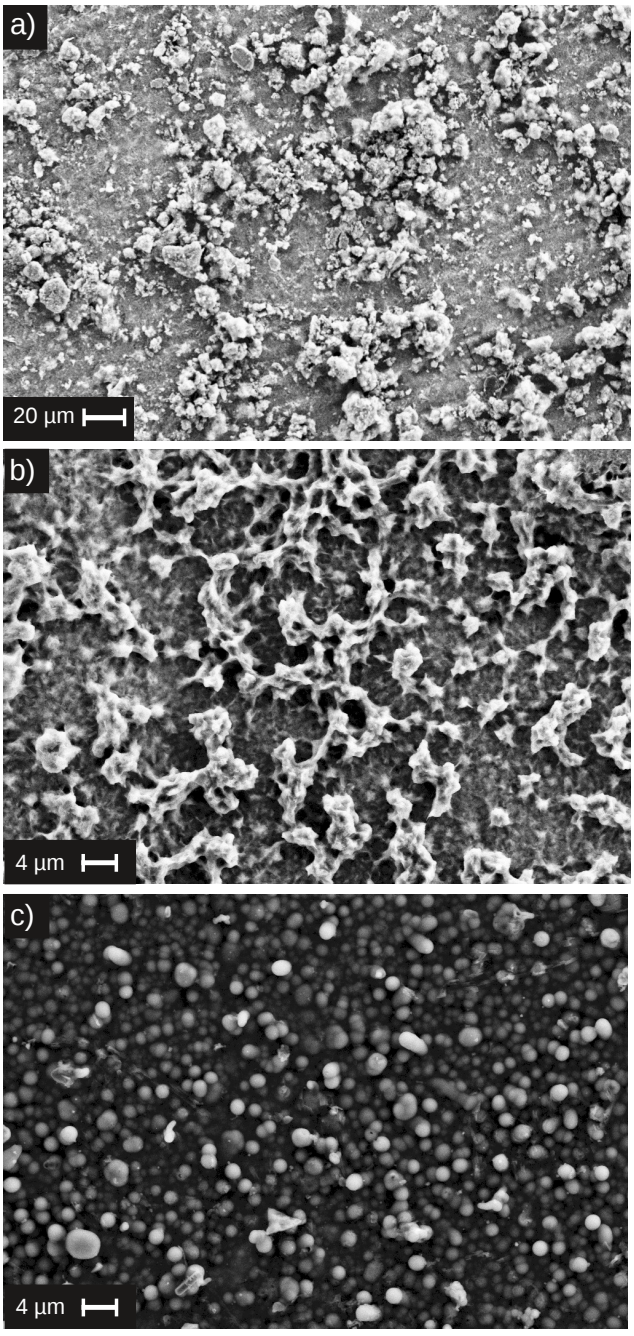

Figure 2: SEM images of the zinc surface after 24 h exposure to (a) 0.1M KCl, (b) 5mM β-CD in 0.1M KCl, and (c) 5mM β-CD[MBT] in 0.1M KCl.

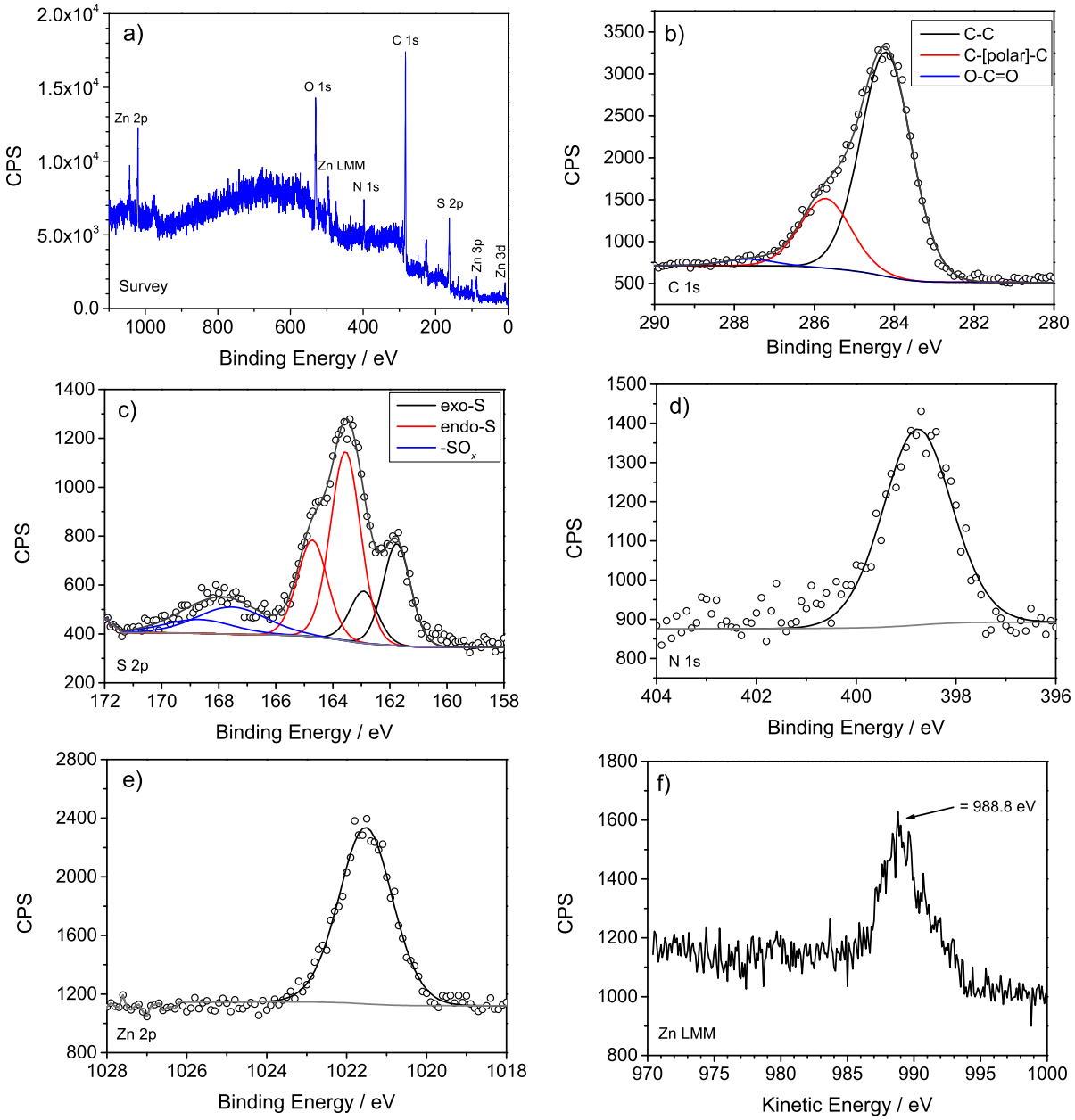

Figure 3: XP spectra of the β-CD[MBT] layer formed on a zinc surface after 24 h exposure of metallic zinc to 5mM β-CD[MBT] in 0.1M KCl. (a) Survey spectrum with major peaks labeled. High resolution spectra in the (b) C 1s, (c) S 2p, (d) N 1s and (e) Zn 2p regions. (f) Zn LMM Auger peak

may be present. Compared to other studies, the intensity of the peak originating from the exocyclic S atom is significantly smaller than expected, which leads to the conclusion that MBT is present in which the exocyclic S-atom is partially oxidized. On the level of energy resolution used in this study, no further conclusions can be drawn on the exact binding state of sulfur, e.g. on its incorporation in an inclusion complex with β-CD. The unlabeled peak in Fig. 3a at 228 eV is most likely the S 1s peak, which won't be discussed here in detail. The Zn 2p region (Figure 3e) is not very sensitive to chemical details of the bond zinc is involved in. The Zn LMM Auger peak position at ≈989 eV shown in Figure 3f shows oxidized zinc in the surface, consistent with the interpretation that significant fractions of ZnO formed.

Delamination of model coatings deposited on pretreated zinc

SKP potential line scans have been carried out to investigate the delamination of PVB model coatings from the differently treated surfaces. Figure 4 shows the progress with time of the potential profiles as a function of distance. All curves follow a typical delamination curve. The defect potentials are 300-500 mV lower than the potential of the intact polymer layer. The lower potential corresponds to the potential where zinc is actively corroding, and the higher potential is corresponding to intact zones of the coating.[46] From the progress of the inflection point of the curve, the delamination rates have been extracted, which are shown in Figure 5. Figure 4a shows the delamination curve of a PVB coating on zinc exposed to 0.1M KCl for 24h before deposition. From the slope of the temporal evolution of the position of the delamination front, a delamination rate of (1627±38) µm/h was obtained (Figure 5). As expected, no stop of delamination was observed until the complete sample was delaminated.

In comparison, the β-CD treated surface shows a slightly different potential profile (Figure 4b). The transition from defect potential to the intact potential is not as sharp as it was for the zinc surface pretreated in the absence of β-CD. The shape of the curve with is "intermediate potential" (Figure 4b) has been reported previously in the literature.[47] This

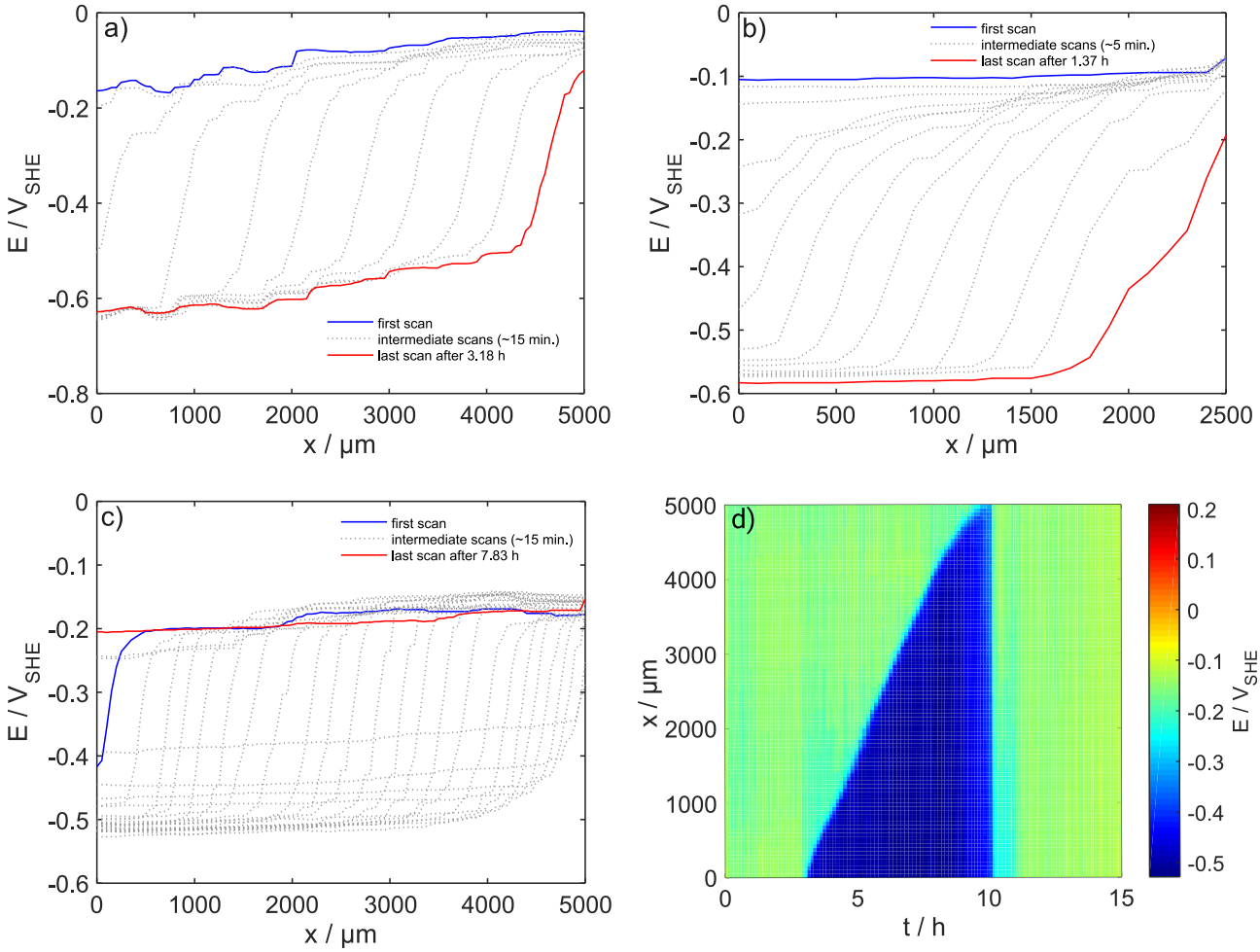

Figure 4: Delamination profile of PVB on (a) an untreated zinc surface, (b) a β-CD modified surface and (c) a β-CD[MBT] modified surface. Figures show the first and the last SKP scan highlighted in red and blue, respectively, and selected intermediate scans. (d) Colour coded potential profile as function of time, including the complete SKP data set on an β-CD[MBT] modified surface. In (a)-(c), time zero has been defined as the last curve on which the potential of the delaminated potential was not visible, while in (d) the complete duration of the experiment is shown.

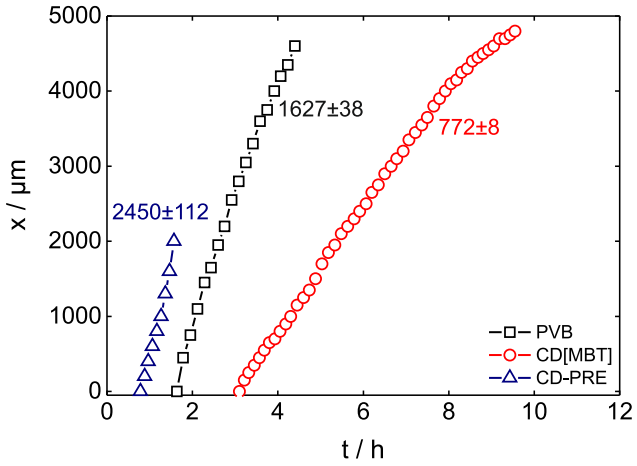

Figure 5: Position of the delamination front as a function of time for the differently treated zinc surfaces. (□) Control experiment of PVB on zinc pretreated in 0.1M KCl. (△) PVB on zinc pretreated in 0.1M KCl + 5mM β-CD. (◯) PVB on zinc pretreated in 0.1M KCl + 5mM β-CD[MBT]. Time zero is defined here as the beginning of the experiment, i.e. when the 1M KCl drop starting the corrosion process was placed on the defect.

curve shape has been associated with a fast diffusion of solvated ions to the metal/coating interface. An explanation for the observed difference to zinc pretreated in the absence of β-CD is that the surface in the presence of β-CD has a different morphology, and becomes more hydrophilic. Therefore, the interfacial region can take up water faster than the system used for comparison. Figure 5 shows the delamination to start earlier compared to the pure PVB system, and the delamination rate to be higher. Higher hydrophilicity also explains the ≈100 mV higher potential compared to PVB on zinc pretreated in the absence of β-CD prior to the start of delamination. Since the experiments were performed in air atmosphere, oxygen reduction at the metal coating interface is occurring, which is likely to be the reason for degradation of the metal-coating bond.[31] From the curve shape observed at the β-CD pretreated surface, the kinetics of the oxygen reduction is deduced to be slower than the ion diffusion of the cations to the interface, which explains the overall shape of the curve profile shown in Figure 4b.[47] As in the case of zinc pretreated in chloride, the delamination does not stop, and the PVB coating completely delaminated over time.

Figure 4c shows the delamination curves for a β-CD[MBT] pretreated sample. A more extensive version of the same data is plotted in Figure 4d. In comparison to the β-CD

pretreated surface, a difference in the shape of the curves is visible. The smooth sigmoidal shape of the curve is an indication that oxygen reduction is faster than the ion diffusion to the interface and is consequently responsible for the degradation of the coating.[47] Compared with the reference surface, the delamination rate is reduced to (772±8) µm/h. Another important point is that the delamination in this system slowed down after about 8 h and stopped subsequently after ≈10 h. The stop of delamination is more obvious in the plot shown in Figure 4d. Slow down and subsequent stop of delamination are a consequence of the increase of the potential in the defect. This potential increase is attributed to the release of MBT from the layer. The MBT reacts with zinc in the defect,[35] resulting in a passivation of the surface after ≈10 h.

In addition to the slowest delamination rate and the stop of delamination, the initiation time is longest for the samples pretreated with β-CD[MBT] (Figure 5). The initiation time is the time between start of exposure of the system to 1M KCl and observed onset of the delamination process by SKP. In the case of β-CD pretreated zinc (Figure 5, △), the initiation of the delamination was observed after ≈1 h, as the most rapid one in this study. Cathodic delamination of the untreated surface started after ≈1.5 h (Figure 5, □). On the β-CD[MBT] pretreated surface (Figure 5, ◯), cathodic delamination started after ≈4 h. Onset times have not been studied systematically to the same extend as delamination rates, though one study touched this point for Sn-containing surfaces.[48] In the system studied here, initiation time correlates with delamination rate, though more systematic analysis of large amounts of data would be needed in order to substantiate such a statement.

Mechanistic discussion

The most important observation in this work is the stop of the delamination, which must be caused by the release of MBT during the corrosion process. The solubility of MBT significantly increases with increasing pH,[35] and the pH of the solution coming in touch with the delaminating region does have an alkaline pH.[49] The local increase of the pH as a result

of the oxygen reduction which is taking place underneath the coating will dissolve MBT from the pretreatment layer. Consequently, a reaction between MBT and dissolved Zn^{2+} is possible in the defect, leading to the formation of a passivating MBT complex layer.[50] It is impossible from the evidence presented here to judge whether MBT release is mainly related to the availability of water at the interface, to the changing electrode potential during delamination, or due to the shift in pH.

The role of the β-CD is two-fold in this process. First of all, the β-CD[MBT] complex has a 2-3 times as high solubility than MBT,[35] thus increasing the availability of MBT for corrosion inhibition. As the complex formation constant is on the order of 10^2,[23] the β-CD[MBT] complex is quite weak. Consequently, if MBT is consumed during corrosion inhibition, it is resupplied from the complex. Second, the β-CD[MBT] complex is needed in the initial pretreatment step in order to ensure that incorporation of the MBT into the initial pretreatment layer is obtained. The hydrophobic MBT cannot incorporate into the aqueous corrosion products of zinc, which are forming in chloride during the preparation step of the pretreatment film. While our group has recently reported that β-CD acts as corrosion inhibitor by itself,[27] its inhibition efficiency is rather low at chloride concentrations of 0.5M and above.[51] Consequently, β-CD itself is likely not directly contributing to the inhibition. Importantly, β-CD itself would not lead to a stop of delamination and the observed potential increase (Figure 4c,d).

The β-CD[MBT] complex does in addition contribute to the formation of the observed compact morphology with spherical particles (Fig. 2c). The model polymer coating PVB used here was found to delaminate slower from zinc surfaces covered with zinc oxide in a spherical morphology, compared to other particle shapes.[52] The delamination rate difference was a factor of 10 for systems with comparable chemical composition.[52] The differences in delamination rate observed in this work may therefore be caused by the differences in morphology between the different surfaces study. However, the morphological differences would naturally not be able to yield the observed increase in defect potential and stop of

delamination (Figure 4c,d). Only the presence of MBT in the system is responsible for this potential increase.

Compared to the previously introduced pretreatment systems based on host-guest complexes between CD and known corrosion inhibitors,[23,25] the system introduced here has the advantage of a simpler synthesis, and the coupling to the intrinsic chemistry of corrosion products forming on zinc. Inhibitor release in the system occurs only if the protection provided by the intrinsic oxide film on zinc breaks down. As described here, the pretreatment with its 24 h pre-corrosion step is not directly suitable for industrial use. However, the phosphating process, which is used industrially to a large extend nowadays, took initially hours to yield passive protecting films.[6] Phosphating is accelerated in modern baths by optimized bath composition, as well as the addition of Ni^{2+}.[5] In the modern nanoceramic conversion coatings, addition of Cu^{2+} yields suitable morphologies and enhanced deposition rates.[53,54] In addition, electrochemical polarisation has been used to accelerate, or even enable, the formation of conversion coatings.[55–58] All these strategies would be applicable to the system introduced here.

Conclusions

A zinc pretreatment has been realized here in which a zinc samples have been pre-corroded in 0.1M KCl containing 5mM of β-CD[MBT] for 24 h. Resulting zinc surfaces show a morphology with oxide-based corrosion products arranged in spherical particles on the surface. XPS shows the presence of nitrogen and sulfur, indicating the presence of MBT on zinc. The so pretreated samples were coated with the model polymer coating PVB. Delamination from defects in the model coating initiated later and progressed slower than in comparable control samples without MBT, and as opposed to these, the defect healed on the time scale of several hours. Defect healing was detected by a potential increase in the defect, which led to a concomitant slow down in delamination rate before the stop of the delamination process.

Stop of delamination has been attributed by the release of MBT via the β-CD[MBT] complex. While the pretreatment step is currently to slow for direct industrial application, this work shows that complexes between CDs and corrosion inhibitors can be incorporated into pretreatments, and triggered release of the inhibitors can stop delamination of a polymer model coating once the coating started to delaminate from a defect. Pretreatments may thus also participate in active corrosion protection.

Acknowledgement

A.A., A.V. and M.R. thank the MPG-FhG project "ASKORR" for funding. A.A. and A.E. acknowledge the DFG (Deutsche Forschungsgemeinschaft) for the financial support of the subproject ER 601/3-1 within priority program 1640 "Joining by plastic deformation". A.S. acknowledges support from the Max Planck Society through the programme Maxnet Energy. Ying-Hsuan Chen is acknowledged for fruitful discussions, and Prof. Stratmann for continuous support.

References

(1) Koch, G.; Varney, J.; Thompson, N.; Moghissi, O.; Gould, M.; Payer, J. *International Measures of Prevention, Application, and Economics of Corrosion Technologies Study*; NACE International: Houston, TX, USA, 2016.

(2) Davis, J. R. *Corrosion - Understanding the Basics*; ASM International: Materials Park, Ohio, USA, 2000; pp 1–20.

(3) Ogle, K.; Buchheit, R. G. In *Encyclopedia of Electrochemistry*; Bard, A., Stratmann, M., Frankel, G., Eds.; Wiley-VCH: Weinheim, Germany, 2007; Vol. 4; Chapter Conversion Coatings, pp 460–499.

(4) Knudsen, O. Ø.; Forsgren, A. *Corrosion Control Through Organic Coatings, Second Edition*; CRC Press: Boca Rayton, USA, 2017.

(5) Rausch, W. *Die Phosphatierung von Metallen, 3rd ed.*; Eugen G. Leuze Verlag: Bad Saulgau, Germany, 2005; pp 15-272.

(6) Freeman, D. *Phosphating and metal pretreatment*; Woodhead-Faulkner: Cambridge, UK, 1986; pp 9-120.

(7) Milošev, I.; Frankel, G. S. Review - Conversion Coatings Based on Zirconium and/or Titanium. *J. Electrochem. Soc.* **2018**, *165*, C127–C144.

(8) Kulinich, S. A.; Akhtar, A. S. On conversion coating treatments to replace chromating for Al alloys: Recent developments and possible future directions. *Russ. J. Non-ferr. Met.* **2012**, *53*, 176–203.

(9) Xia, L.; McCreery, R. L. Chemistry of a Chromate Conversion Coating on Aluminum Alloy AA2024-T3 Probed by Vibrational Spectroscopy. *J. Electrochem. Soc.* **1998**, *145*, 3083–3089.

(10) Tuitt, D. Leaching of Chromates from Primers. *Aircr. Eng.* **1967**, *39*, 8–11.

(11) Kulinich, S.; Akhtar, A.; Susac, D.; Wong, P.; Wong, K.; Mitchell, K. On the growth of conversion chromate coatings on 2024-Al alloy. *Appl. Surf. Sci.* **2007**, *253*, 3144 – 3153.

(12) Li, W.-J.; Yang, C.-L.; Chow, K.-C.; Kuo, T.-W. Hexavalent chromium induces expression of mesenchymal and stem cell markers in renal epithelial cells. *Mol. Carcinog.* **2016**, *55*, 182–192.

(13) Crespy, D.; Landfester, K.; Fickert, J.; Rohwerder, M. In *Self-healing Materials*; Hager, M., van der Zwaag, S., Schubert, U., Eds.; Adv. Polym. Sci.; Springer: Cham, Switzerland, 2015; Vol. 273; pp 219–245.

(14) Stankiewicz, A.; Barker, M. B. Development of self-healing coatings for corrosion protection on metallic structures. *Smart Mater. Struct.* **2016**, *25*, 084013.

(15) Tran, T. H.; Vimalanandan, A.; Genchev, G.; Fickert, J.; Landfester, K.; Crespy, D.; Rohwerder, M. Regenerative Nano-Hybrid Coating Tailored for Autonomous Corrosion Protection. *Adv. Mater.* **2015**, *27*, 3825–3830.

(16) Shchukin, D. G.; Zheludkevich, M.; Yasakau, K.; Lamaka, S.; Ferreira, M. G. S.; Möhwald, H. Layer-by-Layer Assembled Nanocontainers for Self-Healing Corrosion Protection. *Adv. Mater.* **2006**, *18*, 1672–1678.

(17) Vimalanandan, A.; Lv, L.-P.; Tran, T. H.; Landfester, K.; Crespy, D.; Rohwerder, M. Redox-Responsive Self-Healing for Corrosion Protection. *Adv. Mater.* **2013**, 6980–6984.

(18) Williams, G.; Geary, S.; McMurray, H. Smart release corrosion inhibitor pigments based on organic ion-exchange resins. *Corros. Sci.* **2012**, *57*, 139–147.

(19) Chen, Y.-H.; Erbe, A. The multiple roles of an organic corrosion inhibitor on copper investigated by a combination of electrochemistry-coupled optical in situ spectroscopies. *Corros. Sci.* **2018**, *145*, 232 – 238.

(20) Crini, G. Review: A History of Cyclodextrins. *Chem. Rev.* **2014**, *114*, 10940–10975.

(21) Davis, M. E.; Brewster, M. E. Cyclodextrin-based pharmaceutics: past, present and future. *Nat. Rev. Drug Discov.* **2004**, *3*, 1023–1035.

(22) Del Valle, E. M. M. Cyclodextrins and their uses: a review. *Process Biochem.* **2004**, *39*, 1033–1046.

(23) Khramov, A. N.; Voevodin, N. N.; Balbyshev, V. N.; Donley, M. S. Hybrid organo-ceramic corrosion protection coatings with encapsulated organic corrosion inhibitors. *Thin Solid Films* **2004**, *447-448*, 549–557.

(24) Khramov, A. N.; Voevodin, N. N.; Balbyshev, V. N.; Mantz, R. A. Sol–gel-derived corrosion-protective coatings with controllable release of incorporated organic corrosion inhibitors. *Thin Solid Films* **2005**, *483*, 191–196.

(25) Amiri, S.; Rahimi, A. Anticorrosion behavior of cyclodextrins/inhibitor nanocapsule-based self-healing coatings. *J. Coat. Technol. Res.* **2016**, *13*, 1095–1102.

(26) Liu, Y.; Zou, C.; Yan, X.; Xiao, R.; Wang, T.; Li, M. β-Cyclodextrin Modified Natural Chitosan as a Green Inhibitor for Carbon Steel in Acid Solutions. *Ind. Eng. Chem. Res.* **2015**, *54*, 5664–5672.

(27) Altin, A.; Krzywiecki, M.; Sarfraz, A.; Toparli, C.; Laska, C.; Kerger, P.; Zeradjanin, A.; Mayrhofer, K. J. J.; Rohwerder, M.; Erbe, A. Cyclodextrin inhibits zinc corrosion by destabilizing point defect formation in the oxide layer. *Beilstein J. Nanotechnol.* **2018**, *9*, 936–944.

(28) Zhang, X. *Corrosion and Electrochemistry of Zinc*; Plenum Press: New York, 1996.

(29) Fernández-Solis, C. D.; Vimalanandan, A.; Altin, A.; Mondragón-Ochoa, J. S.; Kreth, K.; Keil, P.; Erbe, A. In *Soft Matter at Aqueous Interfaces*; Lang, P. R., Liu, Y., Eds.; Lecture Notes in Physics 917; Springer International Publishing, 2016; pp 29–70, DOI: 10.1007/978-3-319-24502-7_2.

(30) Leidheiser Jr., H.; Wang, W.; Igetoft, L. The mechanism for the cathodic delamination of organic coatings from a metal surface. *Prog. Org. Coat.* **1983**, *11*, 19–40.

(31) Stratmann, M.; Leng, A.; Fürbeth, W.; Streckel, H.; Gehmecker, H.; Große-Brinkhaus, K.-H. The scanning Kelvin probe; a new technique for the in situ analysis of the delamination of organic coatings. *Prog. Org. Coat.* **1996**, *27*, 261–267.

(32) Iqbal, D.; Rechmann, J.; Sarfraz, A.; Altin, A.; Genchev, G.; Erbe, A. Synthesis of Ultrathin Poly(methyl methacrylate) Model Coatings Bound via Organosilanes to Zinc

and Investigation of Their Delamination Kinetics. *ACS Appl. Mater. Interfaces* **2014**, *6*, 18112–18121.

(33) Williams, G.; McMurray, H. N. Chromate Inhibition of Corrosion-Driven Organic Coating Delamination Studied Using a Scanning Kelvin Probe Technique. *J. Electrochem. Soc.* **2001**, *148*, B377–B385.

(34) Williams, G.; McMurray, H. N.; Worsley, D. A. Cerium(III) Inhibition of Corrosion-Driven Organic Coating Delamination Studied Using a Scanning Kelvin Probe Technique. *J. Electrochem. Soc.* **2002**, *149*, B154–B162.

(35) Altin, A.; Rohwerder, M.; Erbe, A. Cyclodextrins as Carriers for Organic Corrosion Inhibitors in Organic Coatings. *J. Electrochem. Soc.* **2017**, *164*, C128–C134.

(36) Liu, C.; Zhao, H.; Hou, P.; Qian, B.; Wang, X.; Guo, C.; Wang, L. Efficient Graphene/Cyclodextrin-Based Nanocontainer: Synthesis and Host–Guest Inclusion for Self-Healing Anticorrosion Application. *ACS Applied Materials & Interfaces* **2018**, *10*, 36229–36239.

(37) Szejtli, J. *Cyclodextrin Technology*; Springer: Dordrecht, 1988; pp. 79-185.

(38) Frankel, G. S.; Stratmann, M.; Rohwerder, M.; Michalik, A.; Maier, B.; Dora, J.; Wicinski, M. Potential control under thin aqueous layers using a Kelvin Probe. *Corros. Sci.* **2007**, *49*, 2021–2036.

(39) Casa Software Ltd, CasaXPS: Processing Software for XPS, AES, SIMS and More. http://www.casaxps.com/.

(40) Thermo Scientific, XPS Simplified. https://xpssimplified.com/periodictable.php.

(41) Wagner, C.; Naumkin, A.; Kraut-Vass, A.; Allison, J.; Powell, C.; Rumble Jr, J. *NIST X-ray photoelectron spectroscopy database; NIST standard reference database 20, version 3.5 (Web version)*; NIST: Gaithersburg, 2007.

(42) Kazansky, L. P.; Pronin, Y. E.; Arkhipushkin, I. A. XPS study of adsorption of 2-mercaptobenzothiazole on a brass surface. *Corros. Sci.* **2014**, *89*, 21 – 29.

(43) Finšgar, M.; Merl, D. K. An electrochemical, long-term immersion, and XPS study of 2-mercaptobenzothiazole as a copper corrosion inhibitor in chloride solution. *Corros. Sci.* **2014**, *83*, 164 – 175.

(44) Kazansky, L.; Selyaninov, I.; Kuznetsov, Y. Adsorption of 2-mercaptobenzothiazole on copper surface from phosphate solutions. *Appl. Surf. Sci.* **2012**, *258*, 6807 – 6813.

(45) Beattie, D. A.; Kempson, I. M.; Fan, L.-J.; Skinner, W. M. Synchrotron XPS studies of collector adsorption and co-adsorption on gold and gold: silver alloy surfaces. *Int. J. Miner. Process.* **2009**, *92*, 162 – 168.

(46) Fürbeth, W.; Stratmann, M. The delamination of polymeric coatings from electrogalvanised steel - a mechanistic approach.: Part 1: delamination from a defect with intact zinc layer. *Corros. Sci.* **2001**, *43*, 207–227.

(47) Wapner, K.; Stratmann, M.; Grundmeier, G. In situ infrared spectroscopic and scanning Kelvin probe measurements of water and ion transport at polymer/metal interfaces. *Electrochim. Acta* **2006**, *51*, 3303–3315.

(48) Wint, N.; Geary, S.; McMurray, H. N.; Williams, G.; de Vooys, A. C. A. The Kinetics and Mechanism of Atmospheric Corrosion Occurring on Tin and Iron-Tin Intermetallic Coated Steels: I. Cathodic Delamination. *J. Electrochem. Soc.* **2015**, *162*, C775–C784.

(49) Iqbal, D.; Sarfraz, A.; Stratmann, M.; Erbe, A. Solvent-starved conditions in confinement cause chemical oscillations excited by passage of a cathodic delamination front. *Chem. Commun.* **2015**, *51*, 16041–16044.

(50) Finšgar, M.; Milošev, I. Inhibition of copper corrosion by 1,2,3-benzotriazole: A review. *Corros. Sci.* **2010**, *52*, 2737 – 2749.

(51) Altin, A. Cyclodextrin for Zinc Corrosion Protection. Ph.D. thesis, Ruhr-Universität Bochum, Bochum, Germany, 2017.

(52) Iqbal, D.; Moirangthem, R. S.; Bashir, A.; Erbe, A. Study of polymer coating delamination kinetics on zinc modified with zinc oxide of different morphologies. *Mater. Corros.* **2014**, *65*, 370–375.

(53) Sarfraz, A.; Posner, R.; Lange, M. M.; Lill, K.; Erbe, A. Role of Intermetallics and Copper in the Deposition of ZrO_2 Conversion Coatings on AA6014. *J. Electrochem. Soc.* **2014**, *161*, C509–C516.

(54) Adhikari, S.; Unocic, K.; Zhai, Y.; Frankel, G.; Zimmerman, J.; Fristad, W. Hexafluorozirconic acid based surface pretreatments: Characterization and performance assessment. *Electrochim. Acta* **2011**, *56*, 1912–1924.

(55) Jegannathan, S.; Narayanan, T. S.; Ravichandran, K.; Rajeswari, S. Performance of zinc phosphate coatings obtained by cathodic electrochemical treatment in accelerated corrosion tests. *Electrochim. Acta* **2005**, *51*, 247 – 256.

(56) Kellner, F. J. J.; Schütze, K.; Kreutz, C.; Virtanen, S. Electrochemical and surface analytical study of the corrosion behavior of mild steel with cathodically produced zinc phosphate coating. *Surf. Interface Anal.* **2009**, *41*, 911–917.

(57) Jegannathan, S.; Arumugam, T.; Narayanan, T. S.; Ravichandran, K. Formation and characteristics of zinc phosphate coatings obtained by electrochemical treatment: Cathodic vs. anodic. *Prog. Org. Coat.* **2009**, *65*, 229–236.

(58) Erbe, A.; Schneider, P.; Gadiyar, C.; Renner, F. U. Electrochemically triggered nucleation and growth of zinc phosphate on aluminium-silicon-coated steel. *Electrochim. Acta* **2015**, *182*, 1132 – 1139.

Graphical TOC Entry